

# A viscoelastic orthotropic Timoshenko beam subjected to general transverse loading

V. Adámek<sup>a,\*</sup>, F. Valeš<sup>b</sup>

<sup>a</sup>Faculty of Applied Sciences, University of West Bohemia, Univerzitní 22, 306 14 Plzeň, Czech Republic

<sup>b</sup>Institute of Thermomechanics, Czech Academy of Sciences, Veleslavínova 11, 301 14 Plzeň, Czech Republic

Received 15 September 2008; received in revised form 19 November 2008

---

## Abstract

The investigation of lateral vibrations of a simply supported thin beam is the aim of this work. The analytical solution of the problem is derived based on the approximate Timoshenko beam theory for a general continuous loading acting on the upper beam face over the whole beam width and perpendicular to the beam axis. The material of the beam studied is assumed linear orthotropic viscoelastic. The generalized standard viscoelastic solid is chosen for representing of viscoelastic beam behaviour. Final system of partial integro-differential equations is solved by the standard method of integral transforms and resulting relations describing beam deflection, slope of the beam and corresponding stress and strain components are presented. Moreover, the derivation of final functions of beam deflection and slope of the beam for a specific impulse loading is presented and analytical results are compared with results obtained using numerical simulation in 2D (FEM). This confrontation shows very good agreement between results obtained. Furthermore, it was shown that the measure of agreement depends not only on the beam geometry.

© 2008 University of West Bohemia in Pilsen. All rights reserved.

*Keywords:* Timoshenko beam, viscoelasticity, orthotropy, analytical solution, numerical simulation, waves propagation, impulse

---

## 1. Introduction

Many methods for studying standard or inverse problems of waves propagation in solids exist. Numerical methods, the application of which is mainly supported by the rapid development of computers, represent a powerful computational tool for a wide range of engineering problems. But the usage of these methods for studying of waves phenomena in solids is usually connected with a vast volume of data even in cases of solids with simple geometries. Generally, the computation is very time-consuming when we use these methods for investigation of transient waves because the time step of integration has to be very small to avoid waves distortion (see [3]). Moreover, it is very difficult to extract and reveal the explicit manner of wave characteristics and their behaviour from such type of results.

On the other hand, exact analytical methods that are ideal for this purpose can be used only for solving of very simple and often too abstract problems. To enlarge the range of problems that can be solved using methods of analytical nature, mixed analytical-numerical methods and approximate analytical methods were developed. The advantage of analytical-numerical methods in comparison with approximate methods consists in a possibility of their application to more complex problems (mainly in the sense of material behaviour, type of external loading

---

\*Corresponding author. Tel.: +420 377 632 335, e-mail: vadamek@kme.zcu.cz.

etc.). These methods are well discussed in the book [8] in context of elastic waves propagation in anisotropic media. The main benefit of analytical methods that are based on approximate theories and that give very good results under corresponding assumptions lies in the possibility of derivation of required solutions in explicit form. This is very important and useful for further investigation of problem studied. But one should emphasize that it cannot be done for every solved problem and without the support of modern computers and high-end software that enables to make very complicated symbolic operations. The set of problems that are solvable by approximate analytical methods and analytical-numerical methods is especially restricted to problems of thin and thick plates, wall strips, thin beams etc. (see e.g. [5, 7]), however these elements form the basis of complex engineering structures.

The lateral vibration of beams under various types of loading has been studied over many years. Recently, many authors deal with lateral vibration of beams under axial loading (compressive or tensile) in combination with moving or fixed transverse loading, usually of harmonic character ([9, 14, 16] etc.). This great practical interest results from designing of long-span bridges and viaducts of roadways where prestressed beams are very often used. Authors usually used analytical-numerical methods for finding the response of uniform or nonuniform beams to such types of loading. Solutions presented in these works are mainly based on the elementary Bernoulli-Euler beam theory.

Problems of a lateral beam vibration that is caused by a transverse non-stationary loading are studied usually by the help of numerical and experimental methods. These approaches enable the authors to solve problems of complicated material behaviour, e.g. in [12] the transient response of a composite sandwich beam to a low-velocity transverse impact is experimentally investigated using high-speed camera. Hao et al. [6] investigate the dynamic phenomena in a complex 3-D orthogonal woven composite T-beam under sudden transverse impact. Results obtained by FEM simulation are confronted with experimental data and discussed.

When the analytical approach is used for solving these problems, authors usually focus on elastic problems or viscoelastic problems with simple material models. Usuki and Maki in [13] derived a higher-order theory for elastic beams using the Reissner functional and involving the influence of nonlinear warping. As the demonstration of their solution, results of the problem of transverse impact to the edge of a semi-infinite beam are presented. Another impact problem of an elastic beam is solved in [15]. By the use of expansion of transient wave functions in a series of eigenfunctions (wave modes), the authors present the analytical solution of a transient problem of a cantilever beam driven by periodic force and repeatedly impacting against a rod-like stop.

The aim of the current study is to investigate wave phenomena in an orthotropic viscoelastic thin beam subjected to a general stationary or non-stationary transverse loading. This paper is the continuing and the generalization of the work [2], in which the authors present analytical and numerical solutions of non-stationary vibrations of an orthotropic viscoelastic thin beam. The problem in this work was solved as symmetric one and the beam of finite length was subjected to a specific type of transverse pressure loading described by the Heaviside function in time. Resulting analytical solution for beam deflection and slope of the beam are presented in [2], relations for other mechanical quantities are not derived there.

## 2. Problem formulation and governing equations

The geometry of the problem solved is depicted in fig. 1. We will assume a simply supported thin beam of finite length  $l_0$  and of constant rectangular cross-section with height  $d_0$  and width

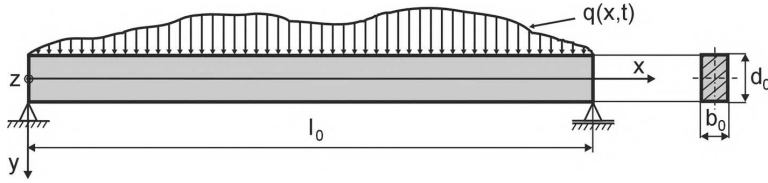


Fig. 1. Geometry of problem solved

$b_0$ . Let us introduce the coordinate system according to the fig. 1. Then we will suppose that the beam is excited by a nonuniform continuous loading  $q(x, t)$ , which remains constant over the whole beam width, i.e. the problem is independent of the coordinate  $z$  and a plane bending problem is solved.

As mentioned in previous section, material properties of the beam are assumed orthotropic and linear viscoelastic. The discrete model of the generalized standard linear viscoelastic solid is used to model such material behaviour in  $x$  and  $y$  directions. This model in  $x$  direction is depicted in fig. 2 with all necessary material parameters.

Elastic constants  $\mu_{xyk}$ ,  $E_{xk}$  and  $G_{xyk}$  for  $k = 0, 1, 2, \dots, N$  represent elastic Poisson's ratio, Young modulus and shear modulus of a specific spring in material model, respectively. The viscous quantities  $\nu_{xyk}$ ,  $\lambda_{xk}$  and  $\eta_{xyk}$  for  $k = 1, 2, \dots, N$  denote viscous Poisson's ratio and coefficients of normal and shear viscosity, respectively. Final form of required constitutive relations was derived under the assumption  $\mu_{ijk} = \nu_{ijk}$  for  $k = 1, 2, \dots, N$  and  $i, j = x, y$  in [2]. The authors used the same methodology as in one-dimensional problems (see [10]). This approach is not quite exact, it is some type of approximation of material properties, but the usage of the exact two-dimensional material model makes the derivation of the analytical solution much more difficult.

Resulting relations for non-zero stress components  $\sigma_x$  and  $\tau_{xy}$  can be written under the assumption of zero initial conditions in the form [2]

$$\begin{aligned} \sigma_x(x, y, t) &= \left( \sum_{k=0}^N E_{xk} \right) \varepsilon_x(x, y, t) - \sum_{k=1}^N \frac{E_{xk}^2}{\lambda_{xk}} \int_0^t \varepsilon_x(x, y, \tau) e^{-\frac{E_{xk}}{\lambda_{xk}}(t-\tau)} d\tau, \\ \tau_{xy}(x, t) &= \left( \sum_{k=0}^N G_{xyk} \right) \gamma_{xy}(x, t) - \sum_{k=1}^N \frac{G_{xyk}^2}{\eta_{xyk}} \int_0^t \gamma_{xy}(x, \tau) e^{-\frac{G_{xyk}}{\eta_{xyk}}(t-\tau)} d\tau. \end{aligned} \quad (1)$$

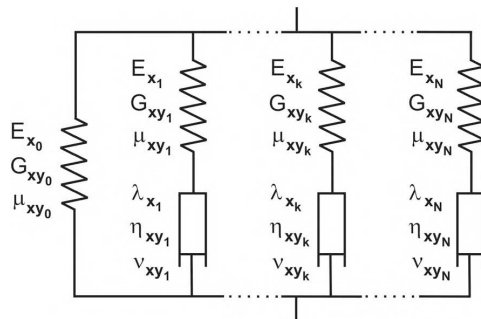


Fig. 2. Scheme of material model used

Motion equations describing lateral vibrations of the beam studied can be easily derived from motion equations stated in [2]. Mentioned equations were derived under the assumption of small strains and on the basis of the approximate Timoshenko beam theory, so the influence of rotary inertia on beam deflection and shear effects were taken into account. No warping of a beam cross-section was involved. Using geometric and material parameters from fig. 1 and fig. 2 and equations stated in [2], final motion equations for the problem solved can be written in the form

$$\begin{aligned}
 d_0^2 \left[ \rho \frac{\partial^2}{\partial t^2} \alpha(x, t) - \left( \sum_{k=0}^N E_{x_k} \right) \frac{\partial^2}{\partial x^2} \alpha(x, t) + \sum_{k=1}^N \frac{E_{x_k}^2}{\lambda_{x_k}} \int_0^t \left( \frac{\partial^2}{\partial x^2} \alpha(x, \tau) \right) e^{-\frac{E_{x_k}(t-\tau)}{\lambda_{x_k}}} d\tau \right] + \\
 + 12 \kappa \left[ \sum_{k=1}^N \frac{G_{xy_k}^2}{\eta_{xy_k}} \int_0^t \left( -\alpha(x, \tau) + \frac{\partial}{\partial x} v(x, \tau) \right) e^{-\frac{G_{xy_k}(t-\tau)}{\eta_{xy_k}}} d\tau - \right. \\
 \left. - \left( \sum_{k=0}^N G_{xy_k} \right) \left( -\alpha(x, t) + \frac{\partial}{\partial x} v(x, t) \right) \right] = 0, \\
 b_0 d_0 \left\{ \rho \frac{\partial^2}{\partial t^2} v(x, t) - \kappa \left[ \left( \sum_{k=0}^N G_{xy_k} \right) \left( -\frac{\partial}{\partial x} \alpha(x, t) + \frac{\partial^2}{\partial x^2} v(x, t) \right) - \right. \right. \\
 \left. \left. - \sum_{k=1}^N \frac{G_{xy_k}^2}{\eta_{xy_k}} \int_0^t \left( -\frac{\partial}{\partial x} \alpha(x, \tau) + \frac{\partial^2}{\partial x^2} v(x, \tau) \right) e^{-\frac{G_{xy_k}(t-\tau)}{\eta_{xy_k}}} d\tau \right] \right\} = q(x, t). \quad (2)
 \end{aligned}$$

Equations (2) represent a system of two partial integro-differential equations of the second order for unknown functions  $v(x, t)$  and  $\alpha(x, t)$ , which describe beam deflection and slope of the beam, respectively. The symbol  $\kappa$  denotes so-called the Timoshenko shear coefficient that involves the influence of shear forces arising in a beam cross-section under bending. Its value depends on the shape of the beam cross-section and for classical shapes can be found for example in [5].

Finally, boundary and initial conditions of the problem solved have to be specified. Appropriate boundary conditions can be easily formulated based on the fig. 1, i.e.  $v(0, t) = 0$  and  $v(l_0, t) = 0$ . Initial conditions for unknown functions and their derivatives will be assumed zero for simplicity.

### 3. Solving of the problem with general loading

In this section, the problem with general external loading  $q(x, t)$  will be solved using the classical method of integral transforms [4]. This method was chosen with respect to some experience acquired by authors by solving similar wave problems (see e.g. [1]).

#### 3.1. Derivation of relations for displacement components

Firstly, the system of partial integro-differential equations (2) will be transformed into the system of partial differential equations using the Laplace transform in time domain. Let us introduce complex integral transforms  $V(x, p) = \mathcal{L}\{v(x, t)\}$  and  $A(x, p) = \mathcal{L}\{\alpha(x, t)\}$ , where  $p \in \mathbb{C}$ . Under the assumption of zero initial conditions, the system (2) can be transformed into

the following system:

$$b_0 d_0 \left[ \rho p^2 V(x, p) - \kappa G^*(p) \left( -\frac{\partial}{\partial x} A(x, p) + \frac{\partial^2}{\partial x^2} V(x, p) \right) \right] = Q(x, p),$$

$$d_0^2 \left( \rho p^2 A(x, p) - E^*(p) \frac{\partial^2}{\partial x^2} A(x, p) \right) - 12 \kappa G^*(p) \left( -A(x, p) + \frac{\partial}{\partial x} V(x, p) \right) = 0, \quad (3)$$

where complex functions

$$E^*(p) = \sum_{k=0}^N E_{x_k} - \sum_{k=1}^N \frac{E_{x_k}^2}{\lambda_{x_k} p + E_{x_k}} \quad \text{and} \quad G^*(p) = \sum_{k=0}^N G_{xy_k} - \sum_{k=1}^N \frac{G_{xy_k}^2}{\eta_{xy_k} p + G_{xy_k}}$$

represent material properties of the beam studied.

The solution of equations (3) and the right-hand side of the first equation will be now assumed in the form of infinite Fourier series. With respect to boundary conditions of the problem, mentioned functions can be expressed as

$$V(x, p) = \sum_{n=1}^{\infty} V_{s_n}(p) \sin \left( \frac{n\pi x}{l_0} \right), \quad (4)$$

$$A(x, p) = \frac{1}{2} A_{c_0}(p) + \sum_{n=1}^{\infty} \left[ A_{c_n}(p) \cos \left( \frac{n\pi x}{l_0} \right) + A_{s_n}(p) \sin \left( \frac{n\pi x}{l_0} \right) \right], \quad (5)$$

$$Q(x, p) = \frac{1}{2} Q_{c_0}(p) + \sum_{n=1}^{\infty} \left[ Q_{c_n}(p) \cos \left( \frac{n\pi x}{l_0} \right) + Q_{s_n}(p) \sin \left( \frac{n\pi x}{l_0} \right) \right]. \quad (6)$$

After the substitution of (4)–(6) into (3), making corresponding derivatives and comparing terms standing by same goniometric functions we obtain equations

$$b_0 d_0 \left\{ -\kappa \frac{n\pi}{l_0} G^*(p) A_{c_n}(p) + \left[ \rho p^2 + \kappa \left( \frac{n\pi}{l_0} \right)^2 G^*(p) \right] V_{s_n}(p) \right\} = Q_{s_n}(p), \quad (7)$$

$$\left\{ d_0^2 \left[ \rho p^2 + \left( \frac{n\pi}{l_0} \right)^2 E^*(p) \right] + 12 \kappa G^*(p) \right\} A_{c_n}(p) - 12 \kappa \frac{n\pi}{l_0} G^*(p) V_{s_n}(p) = 0, \quad (8)$$

$$A_{c_0}(p) = A_{s_n}(p) = 0, \quad Q_{c_0}(p) = Q_{c_n}(p) = 0.$$

Equations (7)–(8) represent a simple system of algebraic equations for unknown complex coefficients  $V_{s_n}(p)$  and  $A_{c_n}(p)$  of Fourier series. Introducing the quantity  $\omega_n = (n\pi)/l_0$  and making notations  $V_{s_n}(p) = V_n(p)$ ,  $A_{c_n}(p) = A_n(p)$  and  $Q_{s_n}(p) = Q_n(p)$ , the solution of (7)–(8) is given as

$$A_n(p) = \frac{H_2(n, p) Q_n(p)}{H_6(n, p)} \quad \text{and} \quad V_n(p) = \frac{H_4(n, p) Q_n(p)}{H_6(n, p)}, \quad (9)$$

where complex functions  $H_2(n, p)$ ,  $H_4(n, p)$  and  $H_6(n, p)$  are defined by relations

$$H_2(n, p) = 12 \kappa \omega_n G^*(p), \quad H_4(n, p) = d_0^2 (\rho p^2 + \omega_n^2 E^*(p)) + 12 \kappa G^*(p),$$

$$H_6(n, p) = b_0 d_0 \left[ (\rho p^2 + \kappa \omega_n^2 G^*(p)) H_4(n, p) - \frac{1}{12} H_2(n, p)^2 \right]. \quad (10)$$

The final form of required functions  $v(x, t)$  and  $\alpha(x, t)$  can be simply derived by the substitution of (9) into (4)–(5) and by the use of the formal inverse Laplace transform notation. We can write:

$$\begin{aligned} v(x, t) &= \sum_{n=1}^{\infty} \sin(\omega_n x) \mathcal{L}^{-1} \left\{ \frac{H_4(n, p) Q_n(p)}{H_6(n, p)} \right\}, \\ \alpha(x, t) &= \sum_{n=1}^{\infty} \cos(\omega_n x) \mathcal{L}^{-1} \left\{ \frac{H_2(n, p) Q_n(p)}{H_6(n, p)} \right\}. \end{aligned} \quad (11)$$

With respect to basic assumptions of the problem solved, the last non-zero displacement component  $u(x, y, t)$  that represents the displacement in  $x$  direction can be simply expressed as  $u(x, y, t) = -y \alpha(x, t)$ .

The Bromwich-Wagner integral defining the inverse Laplace transform and the theorem of residue can be used for further modification of resulting functions (11). But it is not necessary for the derivation of further mechanical quantities and for the evaluation of analytical functions obtained, as will be shown later.

### 3.2. Derivation of relations for strain and stress components

Strain components  $\varepsilon_x$  and  $\gamma_{xy}$  can be simply derived by the substitution of (11) into appropriate deformation equations of the theory of small strains, which can be found for example in [2] or [5]. After that we obtain

$$\begin{aligned} \varepsilon_x(x, y, t) &= y \sum_{n=1}^{\infty} \omega_n \sin(\omega_n x) \mathcal{L}^{-1} \left\{ \frac{H_2(n, p) Q_n(p)}{H_6(n, p)} \right\}, \\ \gamma_x(x, t) &= \sum_{n=1}^{\infty} \cos(\omega_n x) \left[ \omega_n \mathcal{L}^{-1} \left\{ \frac{H_4(n, p) Q_n(p)}{H_6(n, p)} \right\} - \mathcal{L}^{-1} \left\{ \frac{H_2(n, p) Q_n(p)}{H_6(n, p)} \right\} \right]. \end{aligned} \quad (12)$$

Other non-zero strain components  $\varepsilon_y$  and  $\varepsilon_z$  can be expressed analogously to the isotropic problem as the product of strain  $\varepsilon_x$  and the appropriate Poisson's ratio.

Resulting relations for non-zero stress components  $\sigma_x$  and  $\tau_{xy}$  can be derived by introducing relations (12) into constitutive equations (1). Since it concerns only elementary substitution and no further simplifications of resulting relations are possible, they will not be given here.

## 4. Solving of the problem with impact loading

The analytical solution of the solved problem for a specific type of external loading will be derived in this section. Further, results obtained by the use of the approximate analytical approach will be confronted with results of a numerical simulation performed in the FE software MCS.Marc.

The external excitation will be considered non-zero only for  $x \in \langle l - \frac{h}{2}, l + \frac{h}{2} \rangle$ . It will be of an impact-like character in time domain and of a cosine shape in space. We will assume it in the form

$$q(x, t) = b_0 \sigma_a \cos\left(\frac{\pi(x-l)}{h}\right) (H(t) - H(t - t_0)), \quad (13)$$

where  $t_0$  denotes the duration time of the impulse. Other parameters used in (13) are clear from fig. 3.

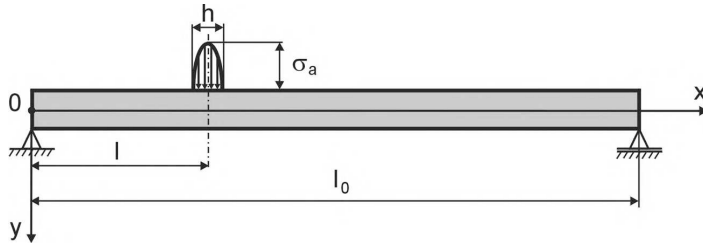


Fig. 3. Geometry of specific problem

4.1. Relations for displacement and strain components

First of all, the appropriate function  $Q_n(p)$  for the loading (13) has to be derived. The Laplace transform of (13) has the form

$$Q(x, p) = b_0 \sigma_a \cos\left(\frac{\pi(x-l)}{h}\right) \frac{1 - e^{-pt_0}}{p}. \tag{14}$$

Then the required sine Fourier coefficient can be expressed as

$$Q_n(p) = \frac{1}{p} C(n) (1 - e^{-pt_0}), \quad \text{where} \quad C(n) = 4 h b_0 \sigma_a \frac{\cos\left(\frac{\pi n h}{2 l_0}\right) \sin\left(\frac{\pi n l}{l_0}\right)}{\pi l_0 \left[1 - \left(\frac{n h}{l_0}\right)^2\right]}. \tag{15}$$

Resulting functions describing spatio-temporal distributions of required displacement components can be then simply derived by the substitution of (15) into (11). Then we can write

$$\begin{aligned} v(x, t) &= \sum_{n=1}^{\infty} C(n) \sin(\omega_n x) \mathcal{L}^{-1} \left\{ \frac{(1 - e^{-pt_0}) H_4(n, p)}{p H_6(n, p)} \right\}, \\ \alpha(x, t) &= \sum_{n=1}^{\infty} C(n) \cos(\omega_n x) \mathcal{L}^{-1} \left\{ \frac{(1 - e^{-pt_0}) H_2(n, p)}{p H_6(n, p)} \right\}, \\ u(x, y, t) &= -y \sum_{n=1}^{\infty} C(n) \cos(\omega_n x) \mathcal{L}^{-1} \left\{ \frac{(1 - e^{-pt_0}) H_2(n, p)}{p H_6(n, p)} \right\}. \end{aligned} \tag{16}$$

Finally, the relations for strain components  $\varepsilon_x$  and  $\gamma_{xy}$  can be obtained by introducing (16) into (12). Then we have

$$\begin{aligned} \varepsilon_x(x, y, t) &= y \sum_{n=1}^{\infty} \omega_n C(n) \sin(\omega_n x) \mathcal{L}^{-1} \left\{ \frac{(1 - e^{-pt_0}) H_2(n, p)}{p H_6(n, p)} \right\}, \\ \gamma_{xy}(x, t) &= \sum_{n=1}^{\infty} C(n) \cos(\omega_n x) \left[ \omega_n \mathcal{L}^{-1} \left\{ \frac{(1 - e^{-pt_0}) H_4(n, p)}{p H_6(n, p)} \right\} - \right. \\ &\quad \left. - \mathcal{L}^{-1} \left\{ \frac{(1 - e^{-pt_0}) H_2(n, p)}{p H_6(n, p)} \right\} \right]. \end{aligned} \tag{17}$$

The evaluation of basic mechanical quantities (16) was made by the help of the system Maple. This software is able to make the symbolic inverse Laplace transform involved in (16)

for specific material and geometric parameters. Moreover, the summation of Fourier series can be done symbolically in this software as well, but not for infinite number of terms. Two thousand of terms were summed to get the analytical solution of required accuracy on the time interval  $t \in \langle 0, 200 \rangle \mu\text{s}$ . The maximum number of terms, which need to be summed, was determined based on the accuracy analysis of analytical solution for very short times ( $t < 1 \mu\text{s}$ ). It was found that this number significantly decreases with increasing time, as could be expected, and that the change of coordinate  $x$  has not so significant influence. Nevertheless, the symbolic summation of 2 000 terms was made for the whole time interval  $t \in \langle 0, 200 \rangle \mu\text{s}$  to obtain one explicit function describing required quantity.

The computation of such one function requires about 400MB of RAM and takes about 4–5 hours on a PC with CPU 3.1 GHz. Functions obtained by this method consist of combinations of a large number of basic goniometric and exponential functions (e.g. the string representing the explicit function of beam deflection contains approximately 1.4mil chars) but the standard mathematical operations (summation, differentiation, integration etc.) can be done with them. Derivation of explicit functions, which describe other mechanical quantities, are then much more simpler and mainly much more faster.

The numerical evaluation of derived spatio-temporal functions was made concretely for following parameters:  $\sigma_a = 10^6 \text{ Pa}$ ,  $l = 30 \text{ mm}$ ,  $h = 3 \text{ mm}$ ,  $l_0 = 100 \text{ mm}$ ,  $d_0 = 5 \text{ mm}$ ,  $\kappa = 0.833$  (this value corresponds to arbitrary rectangular cross-section [5]),  $N = 1$ ,  $\rho = 2250 \text{ kg m}^{-3}$ ,  $\mu_{xy_0} = \mu_{xy_1} = 0.278$ ,  $\eta_{xy_1} = \lambda_{x_1} = 5 \cdot 10^4 \text{ Pa} \cdot \text{s}$ ,  $E_{x_0} = 35 \cdot 10^9 \text{ Pa}$ ,  $E_{x_1} = 18.48 \cdot 10^9 \text{ Pa}$ ,  $G_{xy_0} = 4 \cdot 10^9 \text{ Pa}$ ,  $G_{xy_1} = 18.3 \cdot 10^8 \text{ Pa}$ . The beam dimension  $b_0$  need not to be specified, because the problem is independent of the coordinate  $z$ .

One should emphasize here that some of material parameters used are not real, because it is nearly impossible to find real values of all needed parameters for specific real orthotropic material in literature. Parameters presented by Soden et al. [11] for orthotropic material Gevetex (E-Glass 21xK43) were used as the basis for the estimation of required parameters.

Fig. 4 represents the first analytical results obtained. It shows spatio-temporal distributions of beam deflection and slope of the beam for the impulse loading of duration  $5 \mu\text{s}$  and for intervals  $x \in \langle 0, 100 \rangle \text{ mm}$  and  $t \in \langle 0, 200 \rangle \mu\text{s}$ . If we better explore these resulting surfaces, we find out that reflections of propagated waves from supported beam ends can be observed. Mentioned phenomena are visible in fig. 5 that shows the projection of the surface from figure fig. 4b) to the coordinate plane  $t - x$ .

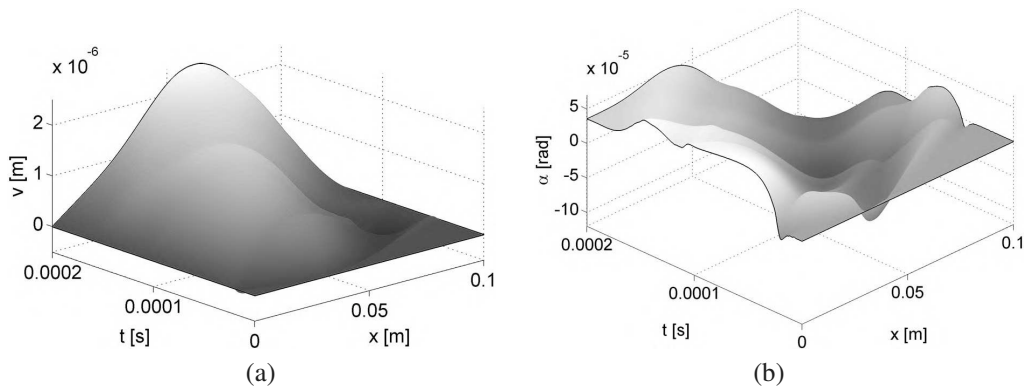


Fig. 4. Spatio-temporal distributions of beam deflection (a) and slope of the beam (b)



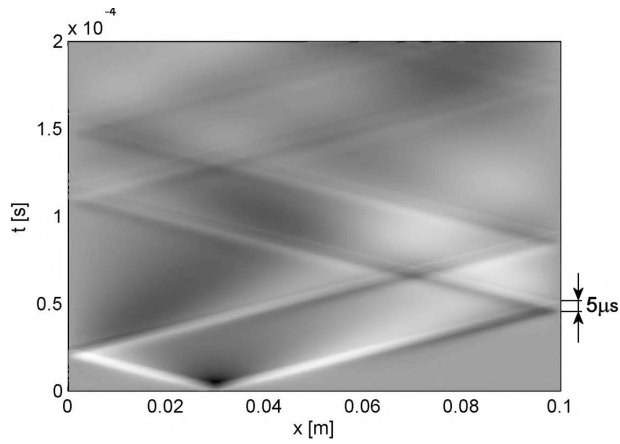


Fig. 5. Reflections of propagated waves (impulse  $5 \mu s$ )

Waves propagation and their reflections are clearly visible in the first half of time interval studied. The dissipation of wave energy is small and wave fronts are steep and markedly visible. After that the dissipation increases and wave fronts become worse distinguishable. Furthermore, unloading waves propagating from the point of excitation when the impulse is terminated (at  $t = 5 \mu s$ ) can be observed from fig. 5. This type of waves can be better seen in fig. 6 where results for impulses taking  $50 \mu s$  and  $100 \mu s$  are presented. Projections of surfaces representing spatio-temporal distribution of strain  $\varepsilon_x$  have to be used to make visible desired wave phenomena. Moreover, additional lights have to be applied, so the levels of grayscale in fig. 6 do not correspond to the value of quantity  $\varepsilon_x$ .

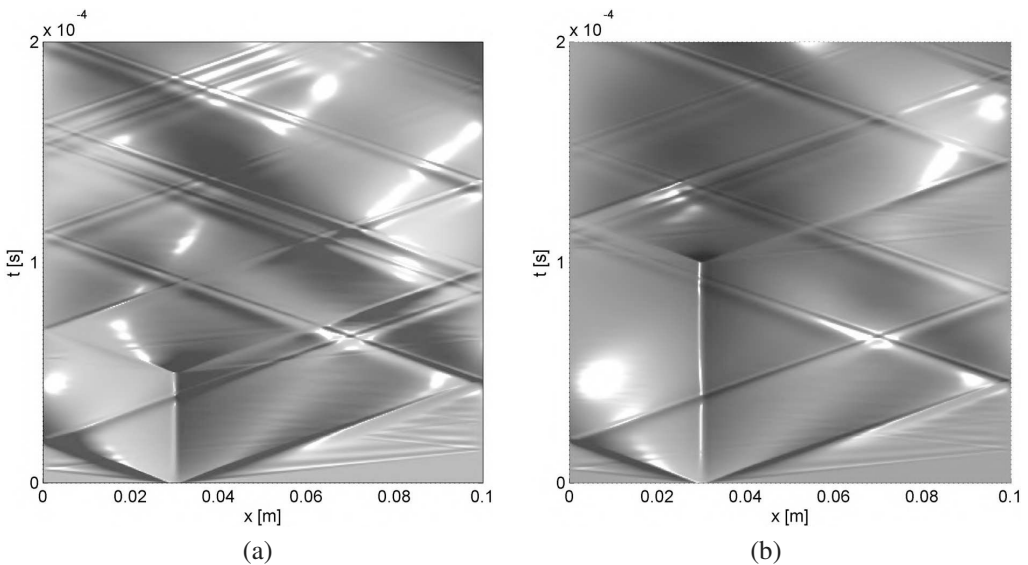


Fig. 6. Reflections of loading and unloading waves for impulses taking (a)  $50 \mu s$  and (b)  $100 \mu s$

#### 4.2. Numerical simulation

The numerical simulation of the problem studied in this section was done using FE software MSC.Marc. The problem was solved as 2D problem of plane stress and four-noded isoparametric elements with linear approximations and with basic dimensions  $0.2 \times 0.2$  mm were used. The beam mesh was regular and only the elements near the area of excitation were once refined to the half size for better representation of applied loading. The size of elements was chosen based on the work [3] and based on experience acquired by authors by numerical simulations of wave phenomena in solids (see e.g. [1, 2]). The boundary condition, which represents simply supported ends of the beam, was defined in two last nodes on the bottom edge of the beam.

Material properties of the beam were represented by the discrete viscoelastic model of the generalized standard viscoelastic solid that is implemented in the software used. Relaxations of Young and shear moduli were prescribed and no volumetric changes of material were assumed. Orthotropic material properties were defined by corresponding elastic material parameters in standard way.

The integration in time domain was performed by the Newmark method with integration step  $2 \cdot 10^{-8}$  s. This value was determined with respect to the maximum stable integration step of the explicit scheme of central differences to avoid waves distortion caused by the omission of high-frequency wave components. This small integration step and the maximum time of interest (200  $\mu$ s) led to relatively time-consuming computation, which took about 26 hours on the same PC that was mentioned in subsection 4.1.

#### 4.3. Results comparison

History plots of beam deflection in several points on the upper edge of the beam will serve for the comparison of analytical and numerical results. Concretely, points with coordinate  $x \in \{30, 35, 40, 60, 80\}$  mm were chosen for this purpose to involve points situated under, close and relatively far from the applied loading.

Fig. 7(a) shows history plots of deflection  $v$  in points of interest within the time interval  $\langle 0, 200 \rangle \mu$ s, which were determined both by analytical (thick lines A.S.) and by numerical (thin lines FEM) approach. These results were obtained for impulse taking  $5 \mu$ s. It is obvious from this figure that both solutions correspond each other quite well in all points studied. Moreover, one can see small oscillations of the numerical solution around the analytical one for  $x = 30$  mm from the detailed view in fig. 7(b). This effect follows on the fact that the point mentioned is situated directly under the external excitation where the 2D (3D) state of stress is developed.

The measure of agreement between both solutions naturally depends on the ratio  $l_0/d_0$ . The greater this ratio is the better agreement between results is obtained. This is demonstrated in fig. 8 that shows history plots of the same quantity as the response to the same type of loading but for beam height  $d_0 = 2$  mm, i.e. the ratio  $l_0/d_0$  is equal to 50. Excellent agreement between analytical and numerical results can be observed both from fig. 8(a) and its detail fig. 8(b).

The authors in [2] have shown that very good agreement between numerical simulations (2D) and the approximate Timoshenko beam theory can be obtained also for  $l_0/d_0 = 10$ . This fact is given by the character of applied loading. Both in this work and in [2], applied loadings have non-stationary characters (the Heaviside function in time was used in [2] and the impulse loading was assumed in this work). However, the excitation in the work mentioned had monotonic character whereas the impulse with loading and unloading behaviour was used in this work. So the measure of agreement between analytical and numerical results depends not only on the geometry of the problem, but also on the type of non-stationary loading.

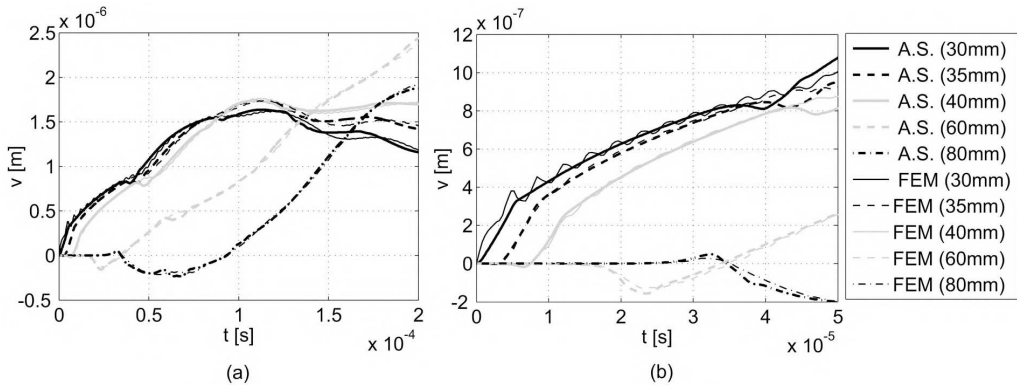


Fig. 7. History plots of deflection  $v$  in points of interest (a) and their detailed view (b) for  $d_0 = 5$  mm

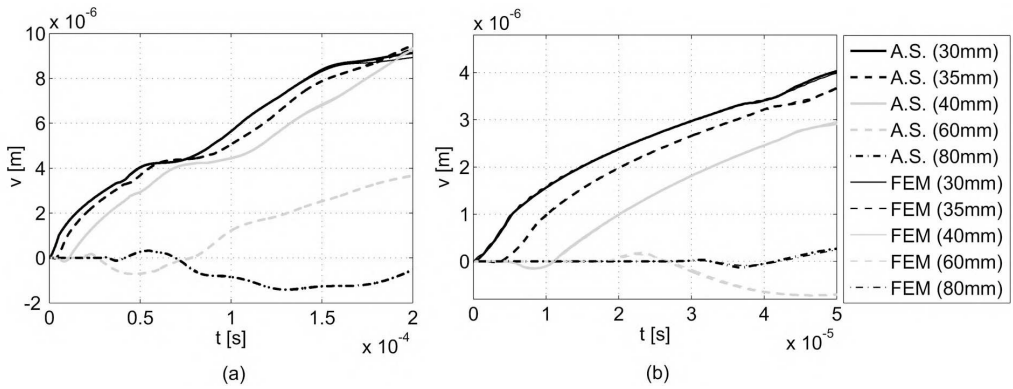


Fig. 8. History plots of deflection  $v$  in points of interest (a) and their detailed view (b) for  $d_0 = 2$  mm

### 5. Conclusion

Non-stationary vibrations of a simply supported thin beam with orthotropic and viscoelastic material behaviour were studied both by analytical and by numerical approach. Firstly, functions representing spatio-temporal distributions of basic mechanical quantities were derived for a general type of continuous transverse loading acting on the upper edge of the beam studied. The Timoshenko beam theory was used for their derivation. In the second part of this work, the specific problem of the beam excited by impact-like loading was solved by analytical and numerical approach. The numerical simulation was done using FEM.

Comparison of results obtained has shown very good agreement of both approaches used for  $l_0/d_0 = 20$  and excellent agreement for  $l_0/d_0 = 50$ . Furthermore, it was shown that the approximate analytical solution of the beam deflection under the applied loading corresponds quite well to results obtained by the FEM simulation that better describes the real problem. The measure of agreement between analytical and numerical results is given not only by the value of the ratio  $l_0/d_0$ , but also by the character of non-stationary excitation (namely, if the loading character is monotonic or not).

The main advantage of analytical approach compared to numerical one consists in the fact that in this case we obtain explicit analytical functions for basic mechanical quantities, which

can be evaluated for arbitrarily large  $x$  or  $t$ , so the study of wave phenomena at arbitrary place and in arbitrary time is possible. Moreover, these functions can be derived for arbitrary geometric parameters (namely large beam length  $l_0$ ), which cannot be always done using FEM under keeping required accuracy for extremely time-consuming numerical computation and for extremely large volume of results. This can be useful for many practical applications.

### Acknowledgements

This work has been supported by the research project MSM 4977751303 and by the grant project GA AS CR A200760611.

### References

- [1] V. Adámek, F. Valeš, V. Laš, Analytical and numerical solution of non-stationary state of stress in a thin viscoelastic plate, *Nonlinear Analysis*, Vol. 63 (2005) e955–e962.
- [2] V. Adámek, F. Valeš, B. Tikal, Non-stationary vibrations of a thin viscoelastic orthotropic beam (in review process for publishing in *Nonlinear Analysis*).
- [3] R. Brepta, F. Valeš, J. Červ, B. Tikal, Rayleigh wave dispersion due to spatial (FEM) discretisation of a thin elastic solid having non-curved boundary, *Computers & Structures* 58 (6) (1996) 1 233.
- [4] D. G. Duffy, *Transform methods for solving partial differential equations*, Chapman & Hall/CRC, Boca Raton, 2004.
- [5] K. F. Graff, *Wave motion in elastic solids*, Clarendon Press, Oxford, 1975.
- [6] A. Hao, B. Sun, Y. Qiu, B. Gu, Dynamic properties of 3-D orthogonal woven composite T-beam under transverse impact, *Composites: Part A* 39 (2008) 1 073–1 082.
- [7] W. Li-li, *Foundations of stress Waves*, Elsevier, Oxford, 2007.
- [8] G. R. Liu, *Elastic waves in anisotropic laminates*, CRC Press, Boca Raton, 2002.
- [9] L. G. Nallim, R. O. Grossi, A general algorithm for the study of the dynamical behaviour of beams, *Applied Acoustic* 57 (1999) 345–356.
- [10] Z. Sobotka, *Rheology of materials and engineering structures*, Elsevier, Amsterdam, 1984.
- [11] P. D. Soden, M. J. Hintomb, A. S. Kaddoura, Lamina properties, lay-up configurations and loading conditions for a range of fibre-reinforced composite laminates, *Composites Science and Technology*, Vol. 58 (1998) 1 011–1 022.
- [12] V. L. Tagarielli, V. S. Deshpande, N. A. Fleck, The dynamic response of composite sandwich beams to transverse impact, *International Journal of Solids and Structures* 44 (2007) 2 442–2 457.
- [13] T. Usuki, A. Maki, Behavior of beams under transverse impact according to higher-order beam theory, *International Journal of Solids and Structures* 40 (2003) 3 737–3 785.
- [14] L. N. Virgin, R. H. Plaut, Effect of axial load on forced vibrations of beams, *Journal of Sound and Vibrations* 168 (1993) 395–405.
- [15] X. C. Yin, Y. Qin, H. Zou, Transient responses of repeated impact of a beam against a stop, *International Journal of Solids and Structures* 44 (2007) 7 323–7 339.
- [16] X. Q. Zhu, S. S. Law, Precise time-step integration for the dynamic response of a continuous beam under moving loads, *Journal of Sound and Vibrations* 240 (2000) 962–970.